Density functional study of ⟨110⟩-oriented thin silicon nanowires

Pavel B. Sorokin,[1,2,3,*] Pavel V. Avramov,[4] Alexander G. Kvashnin,[1] Dmitry G. Kvashnin,[1] Sergey G. Ovchinnikov,[1,2] and Alexander S. Fedorov[2]

[1]*Siberian Federal University, 79 Svobodny Avenue, Krasnoyarsk 660041, Russia*
[2]*Kirensky Institute of Physics, Russian Academy of Sciences, Akademgorodok, Krasnoyarsk 660036, Russia*
[3]*Emanuel Institute of Biochemical Physics, Russian Academy of Sciences, 4 Kosigina Street, Moscow 119334, Russia*
[4]*Fukui Institute for Fundamental Chemistry, Kyoto University, 34-3 Takano Nishihiraki, Sakyo, Kyoto 606-8103, Japan*

The electronic band structure and energetic stability of two types of ⟨110⟩ oriented silicon nanowires terminated by hydrogen atoms are studied using the density functional theory. The nanowires truncated from the bulk silicon with [100] and [111] facets and the pentagonal star-shaped nanowires with [111] facets have the lowest cohesive energies, whereas the hexagonal star-shaped ones are the highest in energy. The star-shaped nanowires have the lowest band gaps with direct and indirect transitions for pentagonal and hexagonal types, respectively. Based on the theoretical results, an interpretation of existing experimental data has been provided.

Silicon nanowires (SiNWs) represent a particularly attractive class of building blocks for nanoelectronics, such as the field-effect transistors (FETs),[1,2] logic gates,[3] and sensors.[4] The effective sizes and electronic properties of the species can be controlled during synthesis in a predictable manner.[5] Some recent studies suggested that SiNW FETs exhibit transport characteristics that are comparable to or exceed those of the best planar devices fabricated by top-down approaches.[2]

At present, a number of perfect one-dimensional silicon nanowires of various shapes and effective sizes have been synthesized under high temperature conditions. The SiNWs grow along a number of crystallographic directions: ⟨100⟩,[6,7] ⟨110⟩,[6–9] ⟨111⟩,[5,8,9] and ⟨112⟩.[8,9] Although the resulting wires are generally covered by oxide layers, complete removal of those oxide layers is possible, leading to SiNWs with hydrogen-passivated surfaces.[6]

Because the exact atomic structure of the SiNWs is unknown in most cases, some theoretical calculations of nanowires with different shapes can be found in the literature. Zhao and Yakobson[10] proposed the pentagonal and hexagonal SiNWs along the ⟨110⟩ direction. Also, the thinnest pristine and covered by oxidized layer pentagonal species have been investigated in detail by Avramov *et al.*[11,12] In particular, the classification of these SiNWs was proposed.[11] The unpassivated and hydrogen-covered ⟨100⟩-oriented SiNWs[13–15] were investigated by *ab initio* methods. Svizhenko *et al.*[16] studied the conductivity of the thinnest SiNWs in ⟨110⟩, ⟨111⟩, and ⟨100⟩ directions. Justo *et al.*[17] reported classical molecular dynamics simulations of pure silicon SiNWs of various shapes and orientations. Marsen *et al.*[18] and Ponomareva *et al.*[19] investigated the thinnest clathrate-based SiNWs.

The main goal of this paper is a theoretical study of hydrogen-covered ⟨110⟩-oriented thin SiNWs, previously discovered experimentally.[6] The atomic and electronic band structure of a set of known,[10,20] as well as newly proposed star-shaped pentagonal and hexagonal ⟨110⟩ oriented thin silicon nanowires, have been calculated using the density functional theory.

The electronic structure calculations of a set of silicon nanowires were carried out using the density functional theory in the framework of the local density approximation[21,22] (LDA) with periodic boundary conditions using the Vienna *ab initio* simulation program (VASP).[23–25] We used a plane-wave (PW) basis set, ultrasoft Vanderbilt pseudopotentials (PP),[26] and a plane-wave energy cutoff equal to 200 eV. To calculate equilibrium atomic structures, the Brillouin zone was sampled according to the Monkhorst–Pack[27] scheme with a $1 \times 1 \times 4$ k-point convergence grid. To calculate the electronic structure, a $1 \times 1 \times 16$ k-point one was used. To avoid interactions between species, neighboring SiNWs were separated by 11 Å in the tetragonal supercells. During atomic structure minimization, structural relaxation was performed until the change in total energy was less than 5×10^{-5} eV/atom or the forces acting on each atom were less than 4×10^{-2} eV/Å. All parameters given above were carefully tested and found to be optimal.

The LDA approximation systematically underestimates the band gap of silicon-based materials by ∼0.6 eV [$E_{\text{gap}}^{\text{calc}}$ =0.6 eV and $E_{\text{gap}}^{\text{expt}}$=1.17 eV (Ref. 28) for the bulk silicon]. The bond lengths were predicted with an accuracy of 3% [$d_{\text{Si-Si}}^{\text{calc}}$=2.18 Å and $d_{\text{Si-Si}}^{\text{expt}}$=2.246 Å (Ref. 29) for Si$_2$ molecule]. It should be mentioned that this result is in good agreement with other *ab initio* calculations (see, for example, Ref. 30).

Classical molecular dynamics (MD) simulations were carried out using the GENERAL UTILITY LATTICE PROGRAM simulation code.[31] The atomic interactions were modeled by the Tersoff many-body potential,[32] which accurately describes the binding energies and elastic properties of a wide range of silicon structures.[17,33]

To study the electronic structure and energetic stability of ⟨110⟩-oriented SiNWs, only high-symmetry and uniformly hydrogen-covered silicon nanowires were calculated using the LDA, PW, and PP methods. Hydrogen passivation prevents reconstruction of the silicon surface according to the Wulff construction rule[34] of minimization of the surface energy and makes the silicon nanowires reveal semiconducting properties.[13]
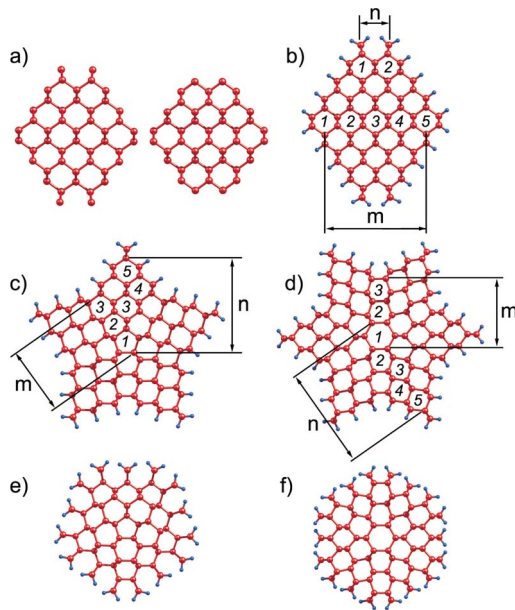
FIG. 1. (Color online) (a) The studied silicon nanowire structures: (a) SiNWTr with (2,5) indices, (b) the pentagonal- and (c) hexagonal star-shaped SiNWs with (5,3) indices, and (d) pentagonal and (e) hexagonal star-shaped SiNW with (3,3) indices.

To study the experimentally observed $\langle 110 \rangle$-oriented nanowires uniformly passivated by SiH_2 groups,[6] two sets of possible structures were calculated. The uniform distribution of hydrogen atoms on the surface assumes that the surface of the resulting structures remains unrelaxed because the relaxation of bare wires yields dramatic surface changes[3] while passivation stabilizes the nanowire structure keeping the tetragonal nature of all silicon atoms.

The SiNWs of the first type can be truncated from the bulk silicon (SiNWTr) with [100] and [111] facets [see Fig. 1(a), with parallel (left) and perpendicular (right) SiH_2 groups orientation to the wire axis. Only SiNWTrs with SiH_2 groups oriented perpendicular to the main axis correspond to the experimentally observed structures[6] and are energetically preferable.[35] Due to these facts, only SiNWTrs with perpendicular SiH_2 groups have been chosen to be theoretically studied in this work.

SiNWTr can be conveniently described in terms of two indices (n, m) defined from the numbers of hexagons in the SiNWTr cross-section parts with minimal (n) and maximal (m) widths. For example, in Fig. 1(b), the (2,5) SiNWTr is shown.

A new type of pentagonal [Fig. 1(c)] and hexagonal [Fig. 1(d)] star-shaped silicon nanowires can be proposed by the combination of five and six $(1, n)$ SiNWTrs, respectively, connecting the constituting parts through equivalent $\langle 111 \rangle$ facets. The resulting objects have 10 and 12 perfect equivalent energetically preferable $\langle 111 \rangle$ facets. Truncation of the edges of the star-shaped nanowires produces [100] facet regions and as the final result gives the pentagonal or hexagonal nanowires proposed by Zhao and Yakobson.[10] The central pentagonal or hexagonal channels of star-shaped wires produce some shared strain but the tubelike surface leads to the lowering of the surface energy and such structures are energetically preferable according to Wulff construction rule for small sized objects.[10]

The proposed pentagonal and hexagonal star-shaped SiNWs also can be described in terms of two indices n and m. The first and second indices correspond to a number of symmetry-irreducible hexagons (plus one center pentagon for pentagonal or one center hexagon for hexagonal wires, correspondingly) in a star arm and body, respectively. For example, in Figs. 1(c) and 1(d), the (5,3) pentagonal and hexagonal star-shaped SiNWs are presented. One can see that the pentagonal and hexagonal SiNW limit structures have (n, n) indices [see, e.g., Figs. 1(e) and 1(f) for (3,3) SiNWs].

We determined the effective size of the studied nanowires as the area of perpendicular cross-section of the species. A similar method has been used in Ref. 17, where the perimeter of SiNWs were used to estimate an effective wire size. Some other methods, such as the determination of a single effective
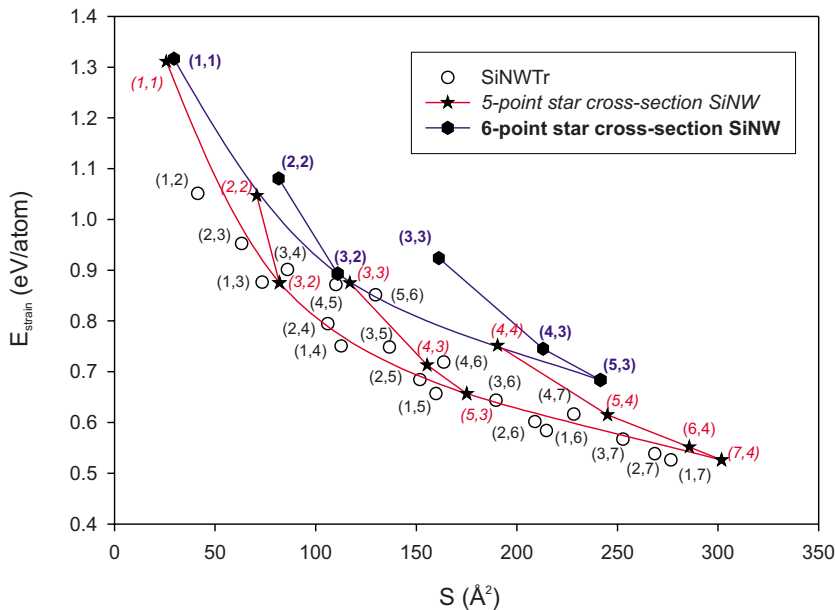
FIG. 2. (Color online) The strain energy (E_{strain}) as function of the SiNW cross-sectional area. The bulk silicon energy is taken as zero. SiNWTrs are marked by empty circles; the pentagonal star-shaped SiNWs are marked by stars with italic type indices; the hexagonal star-shaped SiNWs are marked by hexagons with bold type indices.
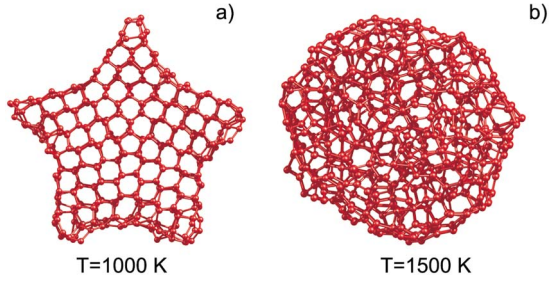
FIG. 3. (Color online) Structural changes in the pentagonal star-shaped SiNW (7,4) in MD simulation at $T = 1000$ K and 1500 K after 100 ps of simulation time.

TABLE I. Comparison of theoretical models and experimental data from Ref. 6.

Nanowire	d_u (Å)	d_w (Å)	E_{gap} (eV)	E_{strain} (eV/atom)
SiNWTr (4,7)	15	29	0.73 (+0.6)	0.07
SiNWTr (4,6)	15	25	0.83 (+0.6)	0.18
Pentagonal (4,4)	15	27	0.70 (+0.6)	0.21
Experimental data[a]	13	26	1.5	

[a]Reference 6.

diameter of a nanowire as the smallest diameter taken from a perpendicular cross-section[31] or the smallest cylinder containing a nanowire,[12,18] are not unambiguous and cannot be applied to species with complex shapes and different facets.

The one-dimensional nature of the wires is also expected to imply a loss of cohesion, at least to a certain degree. The dependence of SiNW strain energies (bulk silicon has zero cohesive energy in this scale) upon the cross-section area is presented in Fig. 2. We would like to mention that the energy of wires truncated from the bulk silicon tends to the bulk value. The star-shaped NWs with infinite diameters should be unstable due to structural tension of central pentagonal or hexagonal channels.

It was found that nanowires with a hexagonal cross section possess the highest energies among all considered SiNWs. The most energetically favorable are the SiNWTrs and pentagonal star-shaped SiNWs. This result is really unexpected because of the strong surface tension of the species

due to the sharp surface of the star arms. Probably it is caused by prohibition of surface reconstruction due to saturation of the surface dangling bonds by hydrogen atoms.

To prove this guess, classical molecular dynamics simulation of hydrogenated and pristine (without hydrogen atoms on the surface) (4,4) (Ref. 10) and (7,4) hexagonal star-shaped silicon nanowires was performed. The energy of hydrogen-covered nanowires is equal to -3.78 eV/atom [for (4,4) SiNW] and -4.04 eV/atom [for (7,4) SiNW], whereas for the pristine nanowires, the cohesive energies are -4.43 eV/atom for (4,4) SiNW and -4.01 eV/atom for (7,4) SiNW. The MD simulations directly show that the surface reconstruction effects play the main role in inversion of the stability of the species under the saturation of dangling chemical bonds, which prevents the reconstruction of the surface and therefore lowering the surface energy.

To study the stability of the species under different conditions, the 100 ps MD simulations of pentagonal star-shaped (7,4) SiNW at $T = 1000$ K and 1500 K were performed. The images of the wire, presented in Fig. 3(a), demonstrate that at
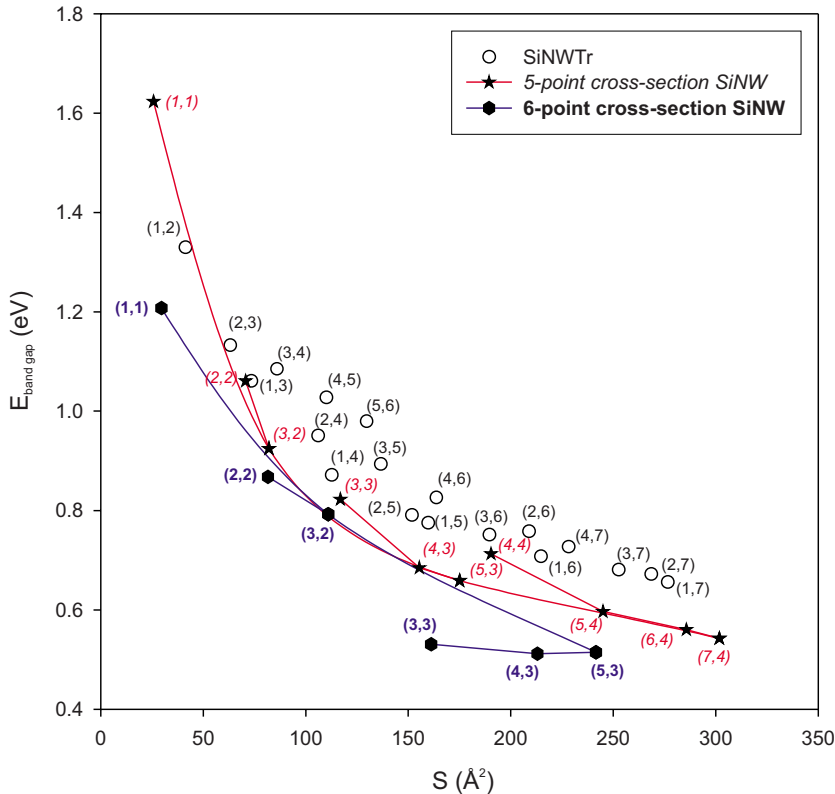
FIG. 4. (Color online) The band gap ($E_{band\ gap}$) of the studied structures as function of the SiNW cross-sectional area. SiNWTrs are marked by empty circles; the pentagonal star-shaped SiNW are marked by stars with italic type indices; the hexagonal star-shaped SiNWs are marked by hexagons with bold type indices.
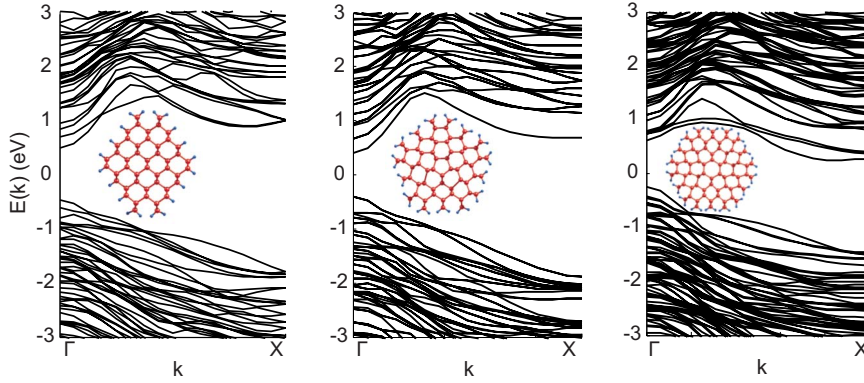
1000 K, the initial shape of (7,4) SiNW does not reveal significant structural changes except for some surface reconstruction. Increasing the temperature (1500 K) transforms the SiNW into tubelike patterns. The polygonal contour of a star-shaped SiNW prevents a transformation to a tubelike one, and only high temperature ($T=1500$ K) creates a smooth contour, along with a completely destroyed nanowire structure [Fig. 3(b)]. In the case of (4,4) SiNW, temperatures of 1000 K already transform the wire to a tubelike structure, according to results of Ref. 10, with smooth surface contour. For other star-shaped species [(5,3) and (9,5) pentagonal SiNW and (7,4) hexagonal SiNW] the MD simulations give similar results.

The dependence of band gap upon the cross-sectional area for all examined nanowires shows the typical $1/d^n$ character[36] of the quantum confinement effect (see Fig. 4), where d is the effective size and n is a fitting parameter, usually ranging from 1 to 2. All SiNWs have the band-gap widths in the range from 0.5 to 1.6 eV. Because of quantum confinement for the thin nanowires, the energy gap is significantly larger the bulk one. The star-shaped nanowires have the lowest band-gap widths among all considered SiNWs. For the thickest size, the band gap of SiNWTr tends toward the bulk value (~0.6 eV). The star-shaped SiNWs display a different situation: their "bulk" value (the interpolation of the area of cross-section of nanowire to infinity) is different (~0.4 eV) from the value of band gap of bulk silicon. This result confirms that such structures cannot exist in the bulk form due to the impossibility of periodicity in directions perpendicular to the wire axis (e.g., in the case of pentagonal star-shaped nanowire, the fivefold symmetry axis is forbidden in crystals). This means that star-shaped nanowires can exist only for finite sizes.

In Fig. 5, the band structures are presented along the wire growth direction. Because of orientation, the features of all bands for all nanowires are similar. All SiNWTrs have a direct band gap [Fig. 5(a)] according to previously reported results.[20,37–39]

In the case of star-shaped SiNWs, the situation is more complicated. The pentagonal SiNWs have a direct band gap [Fig. 5(b)], similar to SiNWTrs, whereas the hexagonal star-shaped SiNWs have an indirect band gap [Fig. 5(c)], with the valence-band maximum located at the Γ point and the conduction-band minimum located approximately at 85%

from Γ to X. Thus, hexagonal SiNWs can evidently be separated from pentagonal SiNWs using optical adsorption experiments.

The STM images of thin $\langle110\rangle$-oriented nanowires[6] reveal the width $d_u=13$ Å of the upper facet with total width of the species about $d_w=26$ Å. There are only three possible structures which can be fitted to the experimental STM image: (4,7), (4,6) SiNWTr, and pentagonal (4,4) SiNW (see Table I). At the LDA PW PP level of theory, the band gaps of these nanowires are equal to 0.73, 0.83, and 0.70 eV, respectively. These values coincide with the experimental data (1.5 eV) taking into account the LDA gap underestimation (~0.6 eV). Since the (4,7) SiNWTr has the lowest energy, this species is the most probable structure discovered in this experiment.[6]

We have examined the stability and electronic properties of two types of $\langle110\rangle$-oriented thin silicon nanowires truncated from the bulk silicon and star-shaped pentagonal and hexagonal structures with [100] and [111] facets. It has been shown that hexagonal star-shaped nanowires are the highest in energy. The pentagonal star-shaped structures and nanowires truncated from the bulk silicon are close in energy and energetically preferable due to prevention of surface reconstruction caused by hydrogen saturation of the dangling bonds. All examined SiNWs reveal band-gap widths in the ranges from 0.5 to 1.6 eV. Comparison of the theoretical band-gap widths with the experimental data[6] shows that the (4,7) SiNWTr is the most probable structure discovered in the experiment.

*Corresponding author. psorokin@iph.krasn.ru

[1] Y. Cui and C. M. Lieber, Science **291**, 851 (2001).

[2] Y. Cui, Z. H. Zhong, D. L. Wang, W. U. Wang, and C. M. Lieber, Nano Lett. **3**, 149 (2003).

[3] Y. Huang, X. Duan, Y. Cui, L. J. Lauhon, K. Kim, and C. M. Lieber, Science **294**, 1313 (2001).

[4] Y. Cui, Q. Wei, H. Park, and C. M. Lieber, Science **293**, 1289 (2001).

[5] A. M. Morales and C. M. Lieber, Science **279**, 208 (1998).

[6] D. D. D. Ma, C. S. Lee, F. C. K. Au, S. Y. Tong, and S. T. Lee, Science **299**, 1874 (2003).

[7] J. D. Holmes, K. P. Johnston, R. C. Doty, and B. A. Korgel, Science **287**, 1471 (2000).

[8] Y. Wu, Y. Cui, L. Huynh, C. J. Barrelet, D. C. Bell, and C. M. Lieber, Nano Lett. **4**, 433 (2004).

[9] V. Schmidt, S. Senz, and U. Gosele, Nano Lett. **5**, 931 (2005).

[10] Y. Zhao and B. Yakobson, Phys. Rev. Lett. **91**, 035501 (2003).

[11] P. V. Avramov, L. A. Chenozatonskii, P. B. Sorokin, and M. S. Gordon, Nano Lett. **7**, 2063 (2007).

[12] P. V. Avramov, A. A. Kuzubov, A. S. Fedorov, P. B. Sorokin, F. N. Tomilin, and Y. Maeda, Phys. Rev. B **75**, 205427 (2007).

[13] R. Rurali and N. Lorente, Phys. Rev. Lett. **94**, 026805 (2005).

[14] A. J. Read, R. J. Needs, K. J. Nash, L. T. Canham, P. D. J. Calcott, and A. Qteish, Phys. Rev. Lett. **69**, 1232 (1992).

[15] M. S. Hybertsen and M. Needels, Phys. Rev. B **48**, 4608 (1993).

[16] A. Svizhenko, P. W. Leu, and K. Cho, Phys. Rev. B **75**, 125417 (2007).

[17] J. F. Justo, R. D. Menezes, and L. V. C. Assali, Phys. Rev. B **75**, 045303 (2007).

[18] B. Marsen and K. Sattler, Phys. Rev. B **60**, 11593 (1999).

[19] I. Ponomareva, M. Menon, D. Srivastava, and A. N. Andriotis, Phys. Rev. Lett. **95**, 265502 (2005).

[20] P. W. Leu, B. Shan, and K. Cho, Phys. Rev. B **73**, 195320 (2006).

[21] P. Hohenberg and W. Kohn, Phys. Rev. **136**, 864 (1964).

[22] W. Kohn and L. J. Sham, Phys. Rev. **140**, 1133 (1965).

[23] G. Kresse and J. Hafner, Phys. Rev. B **47**, 558 (1993).

[24] G. Kresse and J. Hafner, Phys. Rev. B **49**, 14251 (1994).

[25] G. Kresse and J. Furthmuller, Phys. Rev. B **54**, 11169 (1996).

[26] D. Vanderbilt, Phys. Rev. B **41**, 7892 (1990).

[27] H. J. Monkhorst and J. D. Pack, Phys. Rev. B **13**, 5188 (1976).

[28] *Physics of Group IV Elements and III-V Compounds*, Landolt-Börnstein, New Series, Group III, Vol. 17, Part A, edited by O. Madelung (Springer, New York, 1982), and references therein.

[29] K. P. Huber and G. Herzberg, *Constants of Diatomic Molecules* (Van Nostrand Reinhold, New York, 1979).

[30] B.-X. Li, P.-L. Cao, R. Q. Zhang, and S. T. Lee, Phys. Rev. B **65**, 125305 (2002).

[31] J. Gale and A. Rohl, Mol. Simul. **29**, 291 (2003).

[32] J. Tersoff, Phys. Rev. B **38**, 9902 (1988).

[33] H. Zhao, Z. Tang, G. Li, and N. R. Aluru, J. Appl. Phys. **99**, 064314 (2006).

[34] C. Herring, Phys. Rev. **82**, 87 (1951).

[35] R. Rurali, A. Poissier, and N. Lorente, Phys. Rev. B **74**, 165324 (2006).

[36] C. Delerue, G. Allan, and M. Lannoo, Phys. Rev. B **48**, 11024 (1993).

[37] B. Aradi, L. E. Ramos, P. Deák, Th. Köhler, F. Bechstedt, R. Q. Zhang, and Th. Frauenheim, Phys. Rev. B **76**, 035305 (2007).

[38] T. Vo, A. J. Williamson, and G. Galli, Phys. Rev. B **74**, 045116 (2006).

[39] Jia-An Yan, Li Yang, and M. Y. Chou, Phys. Rev. B **76**, 115319 (2007).

[40] http://www.chemcraftprog.com